

https://dspace.org/

Ion transport membrane heat engine integration with autothermal reformingbased methanol production

Phumzile Precious Fankomo; Isabella Greeff

https://hdl.handle.net/10539/41936
WOS

Downloaded from a DSpace repository. https://dspace.org/

Chemical Engineering Research and Design 201 (2024) 307–320

Contents lists available at ScienceDirect

Chemical Engineering Research and Design

journal homepage: www.elsevier.com/locate/cherd

Ion transport membrane heat engine integration with autothermal reforming-based methanol production

Phumzile P. Fankomo, Isabella L. Greeff *

University of the Witwatersrand, School of Chemical and Metallurgical Engineering, 1 Jorissen St, Johannesburg 2000, South Africa

ARTICLE INFO

Keywords:
Ion transport membrane
Autothermal reformer
Syngas
Methanol

ABSTRACT

This study focused on improving the energy demand of conventional large-scale natural gas to methanol flow sheet where even a small efficiency improvement has significant economics and carbon emissions benefits. A conventional flow sheet, case A, was based on best available literature information. A case B where the conventional cryogenic air separation unit (ASU) is replaced with the novel ion transport membrane (ITM) oxygen unit was developed. The ITM oxygen is also heat integrated into the autothermal reformer (ATR) process. A case C where the methanol synthesis process is configured into a gas turbine cycle was developed from further modifying case B. The flow sheets were constructed and modelled in Aspen Plus V10 and, heat and material balance results are reported. To our knowledge, the integration of ITM oxygen membranes into the ATR-based methanol process has not been assessed previously.

Energy and exergy results are generated and analysed. It was found that is it possible to replace the cryogenic ASU with the ITM oxygen for oxygen production in the ATR process. There is enough process syngas heat available to provide the ITM oxygen unit heating requirement and to generate process steam feed to the ATR. Case A was found to consume only 12 % natural gas as utility fuel which is lower than typical SMR-based methanol processes. This reduced to about 5 % in case B and C. Power production improved by 47 % in case B and 68 % in case C compared to case A.

A thermal efficiency definition suitable for combined process steam, power and oxygen production was proposed. This showed that integration of a high temperature gas power cycle enables combined steam (heat) and power configuration which has a higher efficiency compared to single cycles, such as the steam cycles. The overall plant exergy losses decreased by up to 21 %.

1. Introduction and background

Methanol is widely used as an industrial chemical with the end products being ubiquitous in everyday life and in some fuel and electricity sectors. This has led to an increase in the demand and production globally. The largest single methanol plant is in Turkmenistan, Asia, with an installed capacity of 5 225 mt/day (Brelsford, 2020). Larger plants of up to 10 000 mt/day are also being considered, taking advantage of the economy of scale (Aasberg-Petersen et al., 2022). World-wide methanol production capacity exceeded 80 million mt/year in 2021 and is forecasted to exceed 100 million mt/year by 2030.

Natural gas is the largest consumed feedstock in the methanol production industry (Mitsubishi Gas Chemical, 2022) and it is expected that future methanol production expansions will mostly be based on natural gas as a feedstock (Aasberg-Petersen et al., 2022) due to its availability and low cost, as well as its relatively lower waste emissions when compared to coal. The steam-methane reformer (SMR) is used in small-scale conversion of natural gas to syngas. The advantage of the SMR technology is that there is no operating and capital investment cost associated with oxygen production. However, its complex tubular reactor design requires a larger capital investment into the reformer unit and the economy of scale differs significantly with production capacity. The SMR technology is recommended for production capacities of up to 2500 mt/day and oxygen-based technologies are recommended for higher capacities. A two-step SMR followed by oxygen-blown secondary reforming technology is recommended for capacities in the 2500–5000 mt/day range. The auto-thermal reformer technology (ATR)

Abbreviations: ITM, Ion transport membrane; ASU, Air separation unit; ATR, Autothermal reactor; SMR, Steam-methane reactor; WHB, Waste heat boiler; HP, High pressure; MP, Medium pressure; CHP, Combined heat and power; HRSG, Heat recovery steam generator; BFW, Boiler feed water; LHV, Lower heating value.

* Corresponding author.
E-mail address: isabella.greeff@lantic.net (I.L. Greeff).

https://doi.org/10.1016/j.cherd.2023.11.026
Received 11 August 2023; Received in revised form 31 October 2023; Accepted 14 November 2023
Available online 18 November 2023
0263-8762/© 2023 Institution of Chemical Engineers. Published by Elsevier Ltd. All rights reserved.

Nomenclature

Symbols

NG	Natural gas process stream
NGU	Natural gas utility stream
SG	Syngas
FD1	Methanol reactor feed
PG	Purge gas
PD1/PD4	Methanol reactor effluent/Crude methanol product
R2	Recycle stream
W	Work
ΔT_{min}	Minimum heat transfer approach temperature
m	Mass
P	Pressure
T	Temperature
E_d	Exergy destruction
HT3	Methanol reactor feed preheater
HT8	Additional methanol reactor feed preheater
AH	Air heater
Q	Heat duty
Q_C	Heat discharge at low temperature
Q_H	Heat input at high temperature
SGC	Syngas compressor
RC	Recycle compressor
AC	Air compressor
OC	Oxygen compressor
NT	Nitrogen turbine
MRC	Methanol recycle compressor
OT	Oxygen turbine
DM2	Crude methanol separator
HPPH	High pressure steam preheater
HPSUP	High pressure steam superheater
MR	Methanol reactor
MT	Methanol turbine
PC	Product cooler
PH	Preheater
MPSUP	Medium pressure steam superheater

Subscripts

REF	Reforming block
CV	Control volume
i	Inlet
e	Exit
j	Component j

is recommended for greater capacities due to the economy of scale benefit attributed to its simpler design (Blumberg et al., 2017). An example of this is the large ATR-based methanol plant located in Odioma, Nigeria, which will be in operation in 2024 with a capacity of 10 000 mt/day (Air Liquide, 2021).

The ATR technology requires high purity oxygen, which has a high associated capital and energy cost. A typical methanol production process, where a portion of the natural gas is used as utility fuel for power production and process heating, is shown in Fig. 1. In a SMR-based methanol plant, 20 % of the total natural gas feed is typically used as utility fuel (Stanbridge, 2016). The combined syngas and oxygen production accounts for over 60 % of the capital investment (Aasberg-Petersen et al., 2022). The cryogenic air separation unit (ASU) is the only available commercial scale technology for air separation in large-scale applications. The technology is well developed and can achieve high purities of over 99 % and oxygen volumes of up to 50,000 Nm^3/h (Den Exter et al., 2009). The cryogenic ASU however consumes large amounts of energy, mainly for the air compressors. Since the cryogenic ASU is a mature technology, there is little prospect of further drastic improvement and cost reductions (Portillo et al., 2019).

There is a need to improve the thermal efficiency of methanol plants. In large-scale applications even a small improvement in efficiency will have a significant impact on economics. Thermal efficiency improvement may also lead to a reduction in carbon dioxide emissions, as the amount of gas combusted for power and heating may be reduced.

The aim of this study is to develop new conceptual ITM oxygen-based natural gas to methanol flow sheets with improved thermal efficiency for large-scale production processes. A conventional ATR-based methanol process flow sheet is developed based on best available information from literature. Three opportunities for efficiency improvement of this flow sheet are explored.

The first opportunity is the replacement of the cryogenic ASU with an alternative technology, namely ion transport membrane (ITM) oxygen technology. ITM oxygen has the potential to compete with cryogenic ASU as it can produce high purity oxygen at lower cost and power consumption (Kiebach et al., 2022). The technology has been under development since the mid 1990's by Air Products and Ceramatec (Anderson et al., 2016). The technology uses ceramic mixed-metal oxide membranes which are oxygen-ion conducting to separate oxygen from an oxygen-containing gas, such as air. The membranes are operated at high temperatures ranging from 800 to 900 °C (Miller et al., 2014) and can achieve the required purity requirements with acceptable flux rates and reliability (Anderson et al., 2016).

Sunarso et al. (2008) present a review of literature contributions in the development of this technology over the three-decade period, highlighting its potential for high purity oxygen production of up to 100 %. Since the ITM oxygen operates at high temperature, it lends itself to integrate with high temperature processes wherein oxygen and power

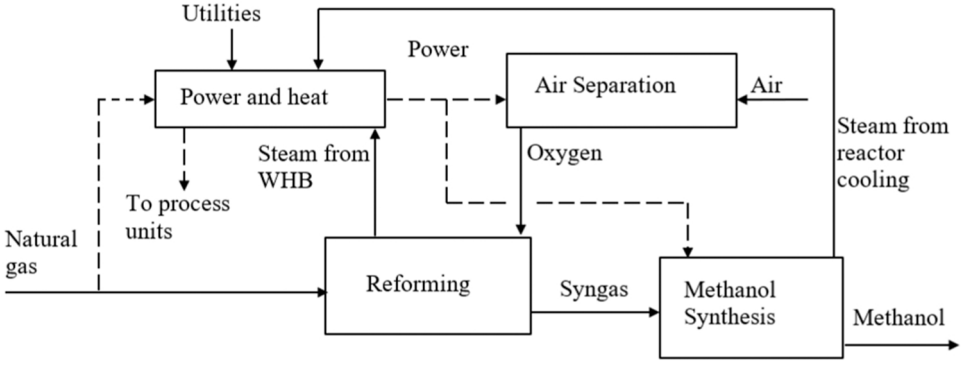

Fig. 1. Schematic diagram of a typical natural gas to methanol process.

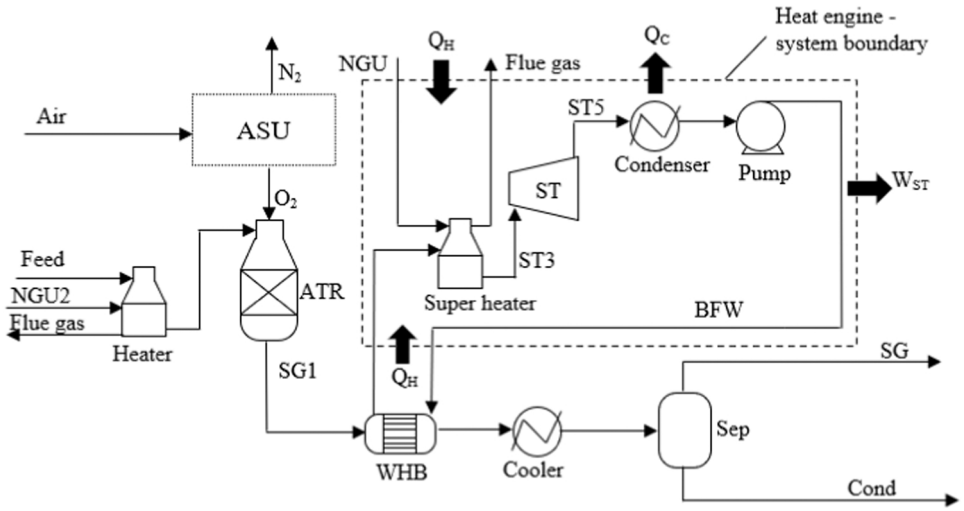

Fig. 2. Schematic diagram of the ATR process coupled with a steam cycle (case A).

are required. Anderson et al. (2016) states that this has been one of the drivers for ongoing developments of the ITM oxygen technology by various research groups. Fischer and Iribarren (2017) found that existing reforming facilities can be upgraded by replacing the conventional cryogenic ASU with the ITM oxygen membranes. The authors found that this can reduce annual costs by 27.3 % in the autothermal reforming of ethanol process.

Recently, Portillo et al. (2019) reported that high capital investment and high energy penalty of the cryogenic ASU in high temperature processes such as the oxy-fuel combustion process hamper its full-scale commercialisation. The ITM oxygen is therefore an alternative to replace the cryogenic ASU. Bai et al. (2021) adds that reasonable process integration enables ITM oxygen systems to show greater advantages in making up for its energy consumption compared to cryogenic ASU. Power output from this system can be increased by adding more heat downstream of the membrane to raise the temperature of the reject stream before expansion. This can be achieved via integration of other available energy sources. The ITM oxygen unit also allows flexibility for further integration of renewable energy, as it is configured like an externally fired gas power cycle where the additional heat from an external source complements co-production of oxygen and power (Greeff, 2022). The external heating source can be nuclear (Greeff, 2015), solar (Habib and Mokheimer, 2017) or biomass. The natural gas feedstock can also be replaced by the use of renewable energy and sustainably sourced materials to produce syngas. For example, the biomass can be gasified to produce carbon monoxide and renewable energy used to produce hydrogen through water electrolysis.

The second opportunity is recovery of heat from the syngas leaving the ATR. In conventional processes, syngas is cooled by generating steam in a waste heat boiler (WHB). This steam is used to generate power, mostly consumed by the cryogenic ASU. The large temperature difference between the steam and syngas leads to high exergy losses as a

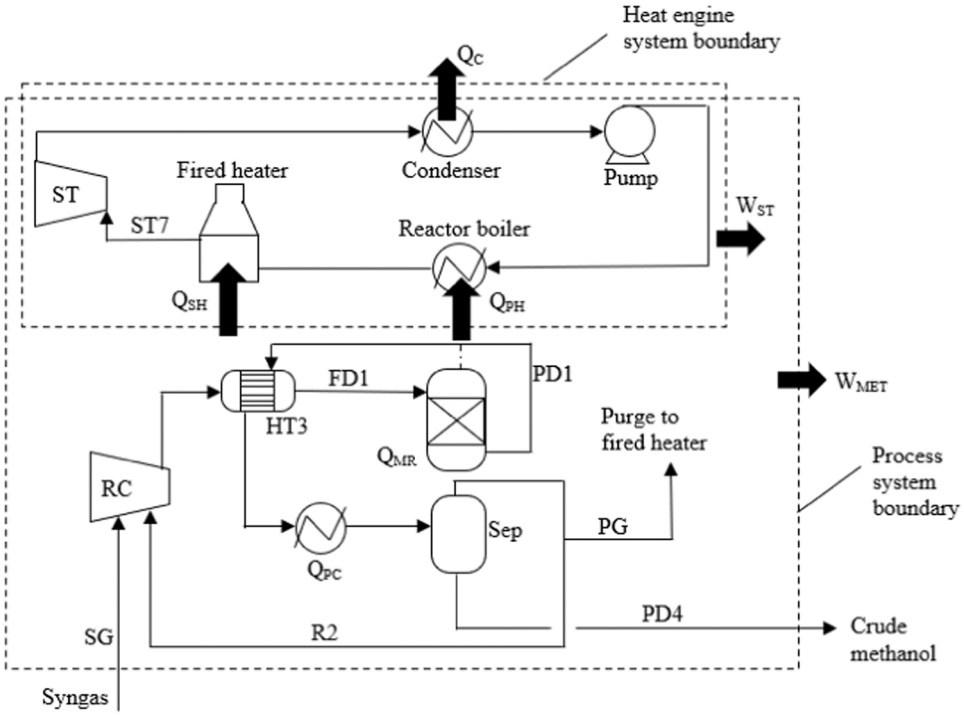

Fig. 3. Conventional methanol synthesis process with steam cycle (case A).

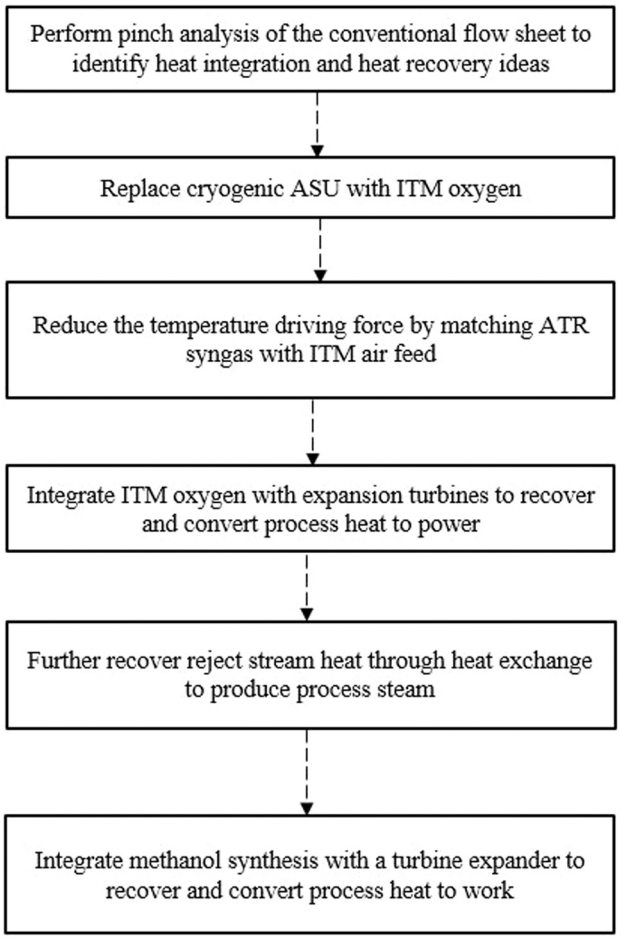

Fig. 4. Flow sheet development approach.

result of degradation of the quality of heat. The amount of power that can subsequently be generated using the process heat, is also reduced, which translates to reduced overall plant thermal efficiency. Iandoli and Kjelstrup, (2007) reports that conventional methods of syngas cooling by generating steam contributes 20 % to overall plant exergy losses for a gas-to-liquids plant comprising ATR technology, low temperature Fischer-Tropsch synthesis and a cryogenic ASU. Various alternative methods to recover or utilize syngas heat have been investigated, including raising the steam pressure in the WHB, direct expansion of the syngas in a turbine expander, feed/effluent heat exchange over the ATR, and gas heated reforming where the syngas heat is used as a heat source for a further steam reforming reactor (Greeff, 2020; Greeff, 2022). An invention by Greeff (2015) presents a process with heat integration of the syngas generation and the ITM oxygen units. In this case, syngas heat is used to further heat the reject stream from the ITM oxygen process to increase the work output from the turbine expander. This is an effective method to recover process heat and was found to improve the thermal efficiency of the power cycle.

The third opportunity is the incorporation of the direct turbine expansion concept in the methanol synthesis loop. The conventional methanol synthesis process is typically heat integrated by heat exchange between the reactor feed and product streams, with an acceptable temperature driving force of ± 30 °C. However, it was shown in previous research work by Greeff et al. (2002) that the net power requirement for syngas compression can be reduced if methanol reaction heat is converted to work by integrating a turbine expander on the outlet of the methanol reactor. In this type of integration, a process gas power cycle with chemical reactor on the high-pressure side, and separation on the low-pressure side of the cycle is created. The high gas recycle rate and high operating pressure of the methanol reactor are exploited to run a gas power cycle using the methanol synthesis loop process gas directly as a working fluid. The integrated system in the study by Greeff et al. (2002) consumes 24 % less power compared to the conventional case. Azadi et al. (2016) elaborated on the concept proposed by Greeff et al. (2002) by applying combined pinch and exergy analysis to such a system. Kotowicz et al. (2022) did a further study on the effect of variation of pressure and temperature on the power production and chemical conversion in a methanol process gas power cycle.

Table 1
Natural gas composition (Venter, 2002).

Natural gas composition (mol%)								
CH_4	C_2H_6	C_3H_8	C_4H_{10}	C_5H_{12}	C_6H_{14}	N_2	CO_2	O_2
94.8	2.6	0.2	0.03	0.01	0.01	1.60	0.81	0.02

In summary, current industrial GTL processes suffer from large energy inefficiencies, making it costly to operate such processes on a large scale. With the increasing demand for methanol and stricter regulations requiring reduced carbon intensity, there is a need to improve sustainability of existing processes. Large exergy losses exist due to poor process heat integration and recovery, mainly in the ATR and ASU processes of conventional large-scale natural gas to methanol plants. Energy improvement can be realized by alternative technologies which integrate heat with the high temperature syngas generation. The ITM oxygen technology has the potential to replace the conventional cryogenic air separation and reduce the large power demands associated with oxygen production. Since the ITM oxygen operates at high temperatures, it requires a source of heat, but also provides the opportunity for energy recovery from the hot permeate and reject streams. The novelty of this work lies in the opportunity to further improve the natural gas to methanol flow sheet by considering the ITM oxygen technology for oxygen production and process heat recovery to improve exergy destruction, reduce energy costs and emissions.

2. Conventional ATR-based methanol production process

2.1. Reforming of natural gas

Fig. 2 shows a conventional ATR process where natural gas is converted to syngas. The steam-methane reforming reaction presented by Eq. 1 below is endothermic, equilibrium driven and occurs at high temperature typically over a nickel-based catalyst (Venter, 2002). The heat required is provided by partial oxidation of methane with

Table 2
Main process information.

Parameter	Value
Reforming block	
Natural gas to ATR	127.9 ton/h
Oxygen to ATR	135.7 ton/h
Process steam to ATR	96.6 ton/h
ATR inlet T	600 °C
ATR operating P	24 bar
ATR outlet T	1036 °C
HP sat steam P	40 bar
HP sup steam T	457 °C
Methanol block	
Dry syngas feed	266.7 ton/h
Methanol reactor P	90 bar
Methanol reactor outlet T	280 °C
Crude methanol	252.3 ton/h
MP sat steam P	10 bar
MP sup steam T	230 °C
Air separation	
Cryogenic ASU power requirement	32 MW
ITM air inlet T	230 °C
ITM operating P	~ 6 bar

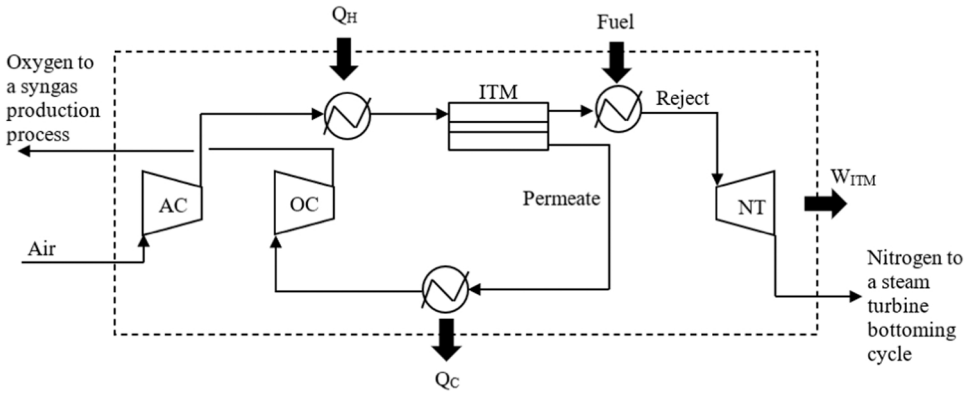

Fig. 5. Heat recovery and conversion to work in an ITM oxygen unit (Anderson et al., 2011).

high-purity oxygen, Eq. 2. The water-gas shift reaction, Eq. 3, adjusts the H_2/CO ratio. The syngas exits the ATR at temperatures in the range of 950–1400 °C (Blumberg et al., 2017). A waste heat boiler (WHB) is used to cool the syngas while generating high pressure (HP) steam. The WHB is integrated into a steam cycle where power is generated from the steam turbine coupled to a generator. The thermal efficiency of these cycles is low, typically at only 33 % (Ramireddy, 2012) and is limited by the temperature at which steam can be produced because of the low critical temperature of water at 374 °C. For material of construction considerations, the steam is generally not superheated to significantly higher temperatures.

Steam-methane reforming reaction (Blumberg et al., 2017)

$$CH_4 + H_2O \leftrightarrow 3\,H_2 + CO \quad \Delta H_0 = 206\ \text{kJ/mol} \tag{1}$$

Partial oxidation reaction (Blumberg et al., 2017).

$$CH_4 + 3/2\,O_2 \rightarrow CO + 2\,H_2O \quad \Delta H_0 = -520\ \text{kJ/mol} \tag{2}$$

Water-gas shift reaction (Blumberg et al., 2017).

$$CO_2 + H_2 \leftrightarrow H_2O + CO \quad \Delta H_{25\,^\circ C,\ 5\ MPa} = 41{\cdot}1\ \text{kJ/mol} \tag{3}$$

2.2. Conventional large-scale oxygen production

The cryogenic air separation process separates gases from air via cooling, liquefaction and distillation. Heat exchangers and distillation columns are very tightly integrated to obtain good efficiency. Specific power consumptions vary from 0.33 kWh/Nm^3 (Beysel, 2009) to 0.38 kWh/Nm^3 (Tesch et al., 2019). There is no scope for heat integration between these units and other blocks in the methanol flow sheet as the ASU's operate at very low temperatures. The units are integrated indirectly with the process via the power obtained from steam generated using process heat.

2.3. Methanol synthesis

Methanol is produced over a copper-based catalyst, that is, copper-zinc oxide with aluminium oxide or chromium (III) oxide Cu-ZnO-Al_2O_3/Cu-ZnO-Cr_2O_3. The selectivity of methanol is over 99 %, thus, side reactions and by-products can be considered negligible (Balopi and Danha, 2019; Greeff et al., 2002; Lucking, 2017). Syngas to methanol reactions are favoured by a higher pressure and lower temperature (Balopi and Danha, 2019) compared to the natural gas reforming process. The main reactions occurring in the methanol reactor are presented in Eqs. 4 and 5 as well as the water-gas shift reaction presented by Eq. 3. The low syngas conversion to methanol rate per pass of only 25 % (Lucking, 2017) necessitates a recycle of the unconverted feed gas.

Hydrogenation of CO and CO_2 (Greeff, 2002; Lucking, 2017).

$$CO + 2\,H_2 \leftrightarrow CH_3OH \quad \Delta H_{25\,^\circ C,\ 5\ MPa} = -90{\cdot}7\ \text{kJ/mol} \tag{4}$$

$$CO_2 + 3\,H_2 \leftrightarrow CH_3OH + H_2O \quad \Delta H_{25\,^\circ C,\ 5\ MPa} = -49{\cdot}5\ \text{kJ/mol} \tag{5}$$

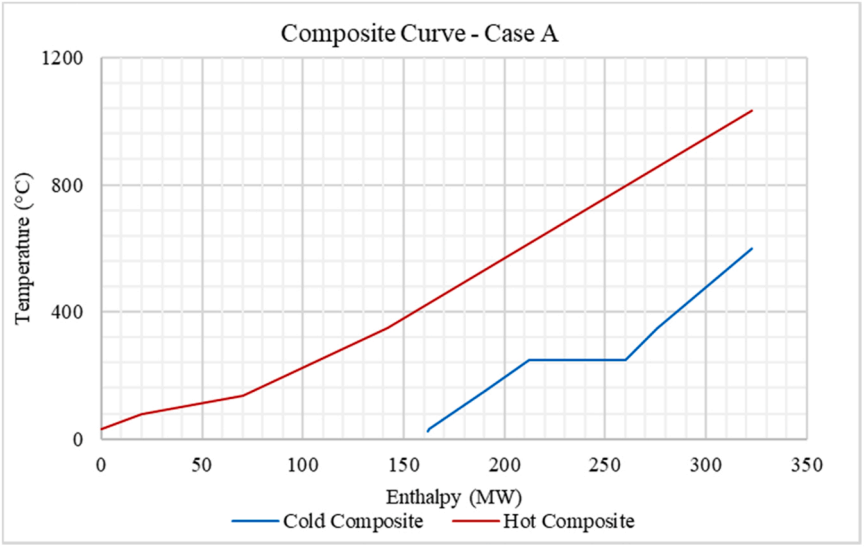

Fig. 6. Composite curves of the conventional ATR flow sheet, excluding cryogenic ASU.

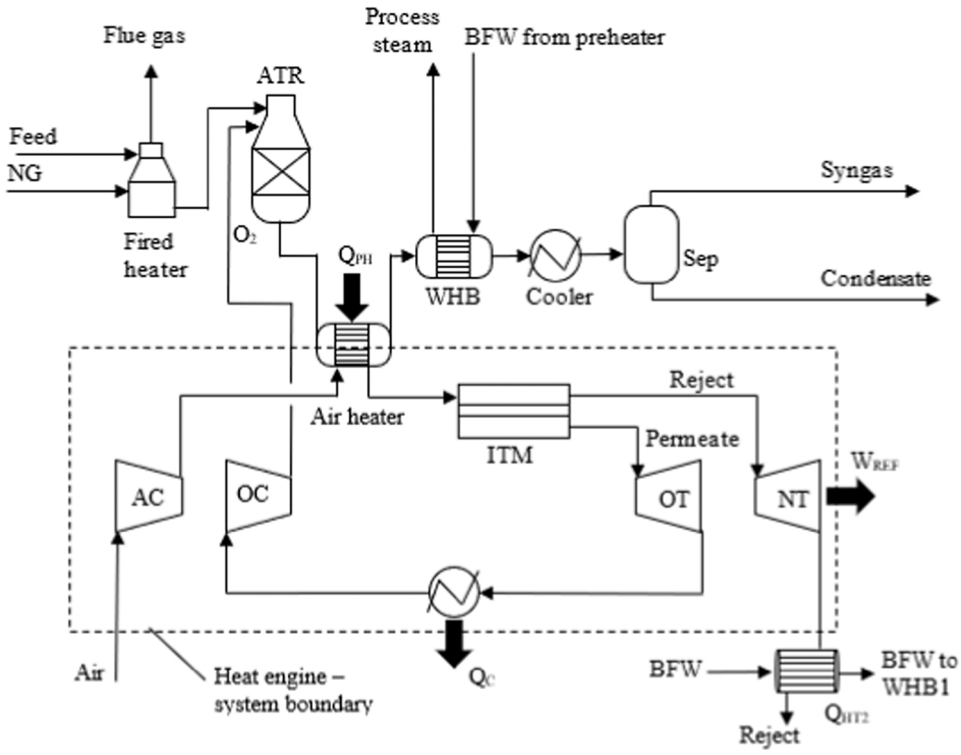

Fig. 7. Integrated ITM oxygen gas power cycle (Case B).

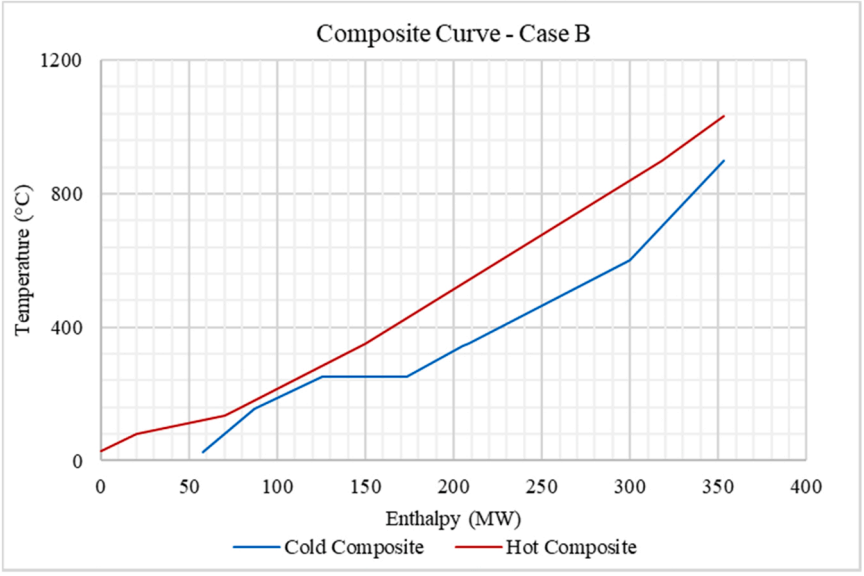

Fig. 8. Composite curves of a new ATR flow sheet including ITM oxygen.

Fig. 3 presents a schematic of a conventional isothermal methanol synthesis process, generating MP steam. The steam is used in a steam power cycle to generate power which is used to supplement the power requirements of the syngas compressor (Greeff, 2002). The purge containing hydrogen can be used as fuel gas for the fired steam superheater.

3. Process flow sheet development and modelling

3.1. Flowsheet development approach

Fig. 4 presents a summary of the steps taken in developing the new flow sheets. The conventional flow sheet, comprising the ATR process configured in Fig. 2 and methanol synthesis process configured in Fig. 3, is named case A. A pinch analysis is performed for case A to compare the typical flow sheet's thermal integration against the theoretical minimum energy targets. A new flow sheet case, whereby the first and second opportunities for improvement are implemented, is named case B. The first opportunity evaluates the replacement of the cryogenic ASU with an alternative technology, namely the ion transport membrane (ITM) oxygen technology. In the second opportunity, recovery of high temperature process heat and conversion to work is evaluated by configuring the ITM oxygen into a power cycle. This has potential to reduce the

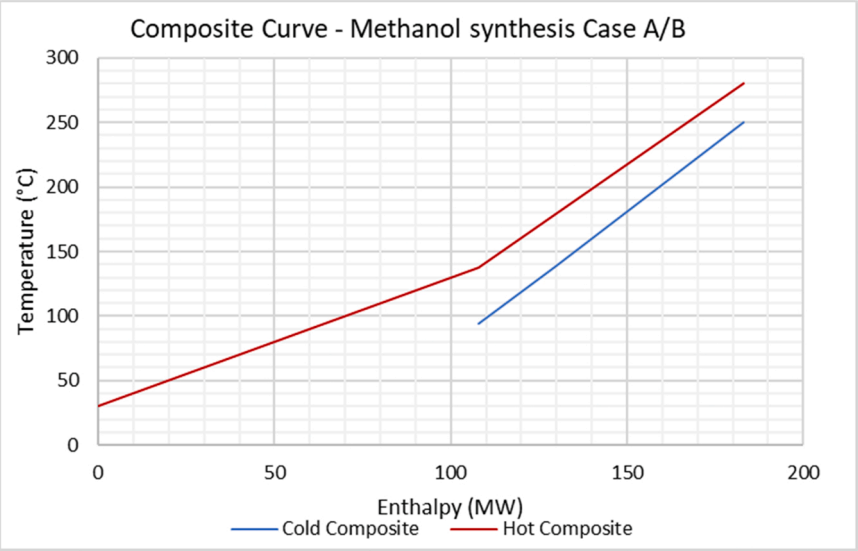

Fig. 9. Composite curves of the conventional methanol synthesis flow sheet case A/B.

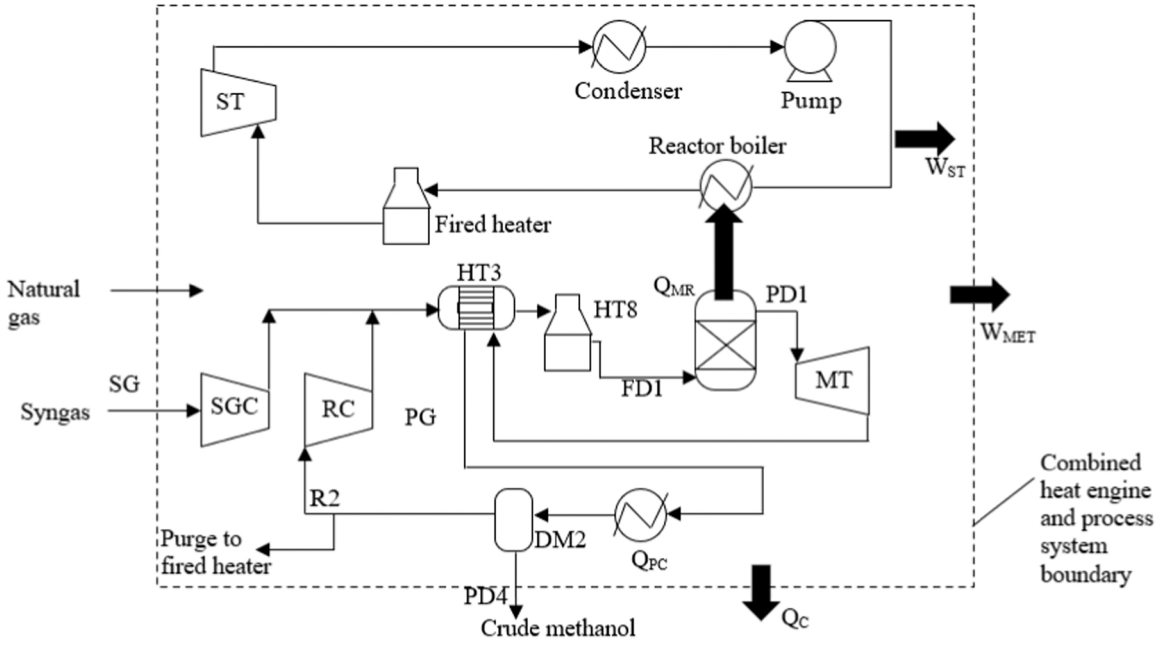

Fig. 10. Integrated methanol process gas power cycle (Case C).

temperature driving forces compared to the conventional process where syngas is cooled in a steam generating waste heat boiler (WHB). A further new flow sheet case whereby the third opportunity for improvement is assessed, is named case C. The third opportunity evaluates the integration of direct turbine expansion in the methanol synthesis loop to convert the methanol reactor effluent heat to work. A resulting improvement in thermal efficiency and increased power production lead to reduced overall energy demand and therefore operating costs for these flow sheets.

3.2. Simulation models

Aspen Plus V10 software was used for the simulation of all flow sheet cases in this work. A suitable Soave-Redlich-Kwong property method was specified in Aspen Plus (Greeff, 2004; Blumberg et al., 2016). The flowrate basis was 5 225 mt/day of methanol production (Brelsford, 2020). Table 1 presents the natural gas composition used.

The assumptions made in the simulation models are as follows:

- The ATR reactor is well insulated and therefore adiabatic.
- There are no long-chain heavy hydrocarbons in the natural gas requiring a pre-reformer.
- There is no sulphur in natural gas requiring sulphur removal.
- There are no double or triple-bond hydrocarbons in the natural gas requiring saturation.
- Line frictional losses are relatively small compared to the flow sheet pressure profile and therefore negligible. Pressure losses through the equipment was also assumed to be negligible compared to pressure changes brought about by compressors and expanders.
- An isentropic efficiency of 85 % was specified for all compressors and turbines.

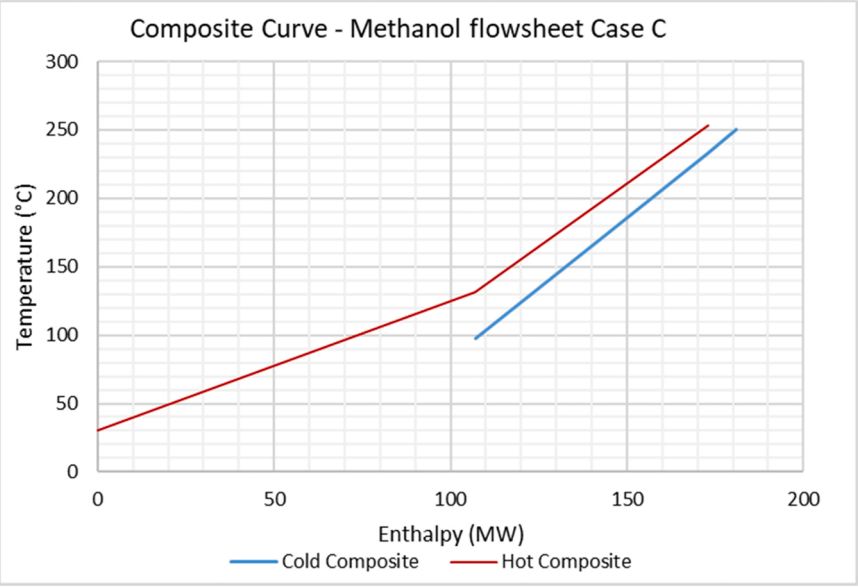

Fig. 11. Composite curves of the new methanol synthesis flow sheet case C.

Table 3
ATR syngas composition (975 °C, 24 bar).

Component	Unit	Syngas composition (Venter, 2002)	Syngas composition in this work	% deviation
CO	mol/mol	0.18	0.17	6 %
H_2	mol/mol	0.39	0.43	10 %
CO_2	mol/mol	0.08	0.08	0 %
H_2O	mol/mol	0.30	0.31	5 %

Table 4
ATR syngas composition (1033 °C, 24 bar).

Component	Syngas composition in this work
CO	0.23
H_2	0.53
CO_2	0.04
H_2O	0.19

The main process information that the simulations are based on are summarised in Table 2.

3.3. ITM oxygen technology integration

In the ITM oxygen separation process, atmospheric air is compressed to the inlet pressure of the membrane separator, typically above 6 bar. The air is then heated using an external heat source before it is fed to the membrane for separation into the reject and permeate streams (Den Exter et al., 2009; Rao and Muller, 2007). The permeate and reject streams are still at high temperature when they exit the membrane separator. Converting this heat to work means the process can be configured as a gas power cycle to co-produce oxygen and power. Fig. 5 presents a high-level diagram of the ITM oxygen process configured to recover energy from the hot reject stream.

Table 5
Syngas to methanol reaction conversion.

	Conversion of Lucking (2017)	Conversion in this work	% deviation
Methanol single pass conversion	0.33	0.30	9 %

Gas power cycles operate at much higher temperatures compared to steam cycles. Fuel is combusted directly with compressed air in typical combustion gas turbine cycles, also known as internally fired cycle. In the case of the ITM oxygen, heat can be transferred from a heat source to the air, which is also known as an externally fired cycle. The thermal efficiency of typical stand-alone gas power cycles is 44.7 % (Langston, 2020). This can be improved by using the heat rejected as a hot utility for process heating, also known as combined heat and power (CHP) production. The steam cycles in the conventional ATR and methanol units are to some extent already being operated as CHP as some of the steam is used as hot utility, and an amount is also used as process feed to the ATR. Another way to improve the low efficiency is to use combined cycles, where a high temperature cycle such as the ITM oxygen power cycle is coupled to a lower temperature cycle such as a steam turbine bottoming cycle via a heat recovery steam generator (HRSG).

Composite curves were used to determine the minimum energy targets. Fig. 6 presents the hot and cold composite curves for the conventional ATR flow sheet, Case A. The methanol synthesis was excluded as it is already subjected to process integration via feed/effluent heat exchange over the reactor. The conventional air separation unit was not included in this pinch analysis due to the cryogenic nature of the process limiting heat integration opportunities.

Minimum heat transfer approach temperatures, ΔT_{min}, of 10 – 20 °C are typically applied in the pinch study of chemical processes. Although a lower ΔT_{min} means more heat recovery and therefore low utility requirements, it comes at an expense on the number of heat exchanger units and heat transfer area. This therefore requires striking a balance between the capital and energy costs when designing the flow sheet. ΔT_{min} of a conventional ATR is high, > 400 °C, if the ATR feed and product are heat integrated via feed/effluent heat exchange. Note the ΔT_{min} is even higher and > 700 °C in a case where water is used to cool syngas, generating steam in a WHB. Such large temperature differences lead to large exergy losses. In case A, the minimum cooling target is 162 MW and the minimum heating target is 0.

In the conventional, ATR process heat integration between the ATR feed and product streams may cause problems with metal dusting corrosion which occurs at such high temperatures and pressures in the presence of carbon compounds (Madloch et al., 2018). Shell however recently filed a patent application attempting to claim feed/effluent heat

Table 6
Stream process conditions and properties.

Stream no.	Case A			Case B			Case C		
	m ton/h	*P* bar	*T* °C	*m* ton/h	*P* bar	*T* °C	*m* ton/h	*P* bar	*T* °C
NG	128	24	30	128	24	30	128	24	30
FD4	225	24	274	225	24	274	225	24	274
O2	136	24	150	136	24	153	136	24	153
NGU	10	24	30	-	-	-	-	-	-
NGU2	6.8	24	30	6.8	24	30	7.5	24	30
SG1	360	24	1033	360	24	1034	361	24	1034
N2	-	-	-	449	1	337	449	1	337
SG	267	24	30	267	24	30	267	24	30
FD1	663	90	250	674	90	250	711	90	250
PD1	663	90	280	674	90	280	711	90	280
R2	396	90	30	407	90	30	445	70	30
PG	14	90	30	15	90	30	16	70	30
ST3	265	40	448	-	-	-	-	-	-
ST7	305	10	229	305	10	230	305	10	226
PD4	252	90	30	252	90	30	250	70	30

Table 7
Thermal and LHV efficiency definitions.

Thermal efficiency of the ITM gas power cycle in Fig. 7	$\eta = \frac{W_{NT} + W_{OT} - W_{AC} - W_{OC}}{Q_{AH}} = \frac{W_{REF}}{Q_{AH}}$	(6)
Thermal efficiency of the steam cycles in Figs. 2 and 3	$\eta = \frac{W_{ST}}{Q_{WHB} + Q_{HPPH} + Q_{HPSUP}}$	(7)
Thermal efficiency of combined steam, oxygen and power system (Case A) Fig. 12	$\eta = \frac{W_{REF} + P_{ST}}{Q_{WHB} + Q_{WHB1} + Q_{HPPH} + Q_{HPSUP} + Q_{HT2} + Q_{HT6}}$	(8)
Thermal efficiency of combined steam, oxygen and power system (Case B) Fig. 13	$\eta = \frac{W_{REF} + P_{ST}}{Q_{AH} + Q_{WHB1}}$	(9)
LHV efficiency (all cases)	$\eta = \frac{LHV_{product} + W_{MET}}{LHV_{feed}}$	(10)
Carbon efficiency	$\eta = \frac{Moles\ of\ methanol\ in\ product}{Moles\ of\ CO\ and\ CO_2\ in\ syngas}$	(11)
Specific gas efficiency	$\eta = \frac{Total\ natural\ gas\ energy\ content}{Methanol\ production\ rate}$	(12)

exchange over an ATR combined with sulphur dosing upstream of the cooling step, to limit metal dusting corrosion (Smit and Sprachman, 2016).

Fig. 7 shows the ATR process with the integrated ITM oxygen unit, case B. Process heat from hot syngas is used to preheat air before entering the ITM. The reject stream is expanded and then used to preheat BFW, which is fed to the smaller WHB for production of process steam. Note that the HP steam cycle is now eliminated. The permeate stream, which is high purity oxygen is expanded, cooled, and compressed again to enable feed to the ATR.

It is important to note that heat integration across the ATR and methanol synthesis units is considered impractical. This is based on the authors' work experience with large-scale gas-to-liquids processes in South Africa, where the ATR and methanol synthesis units are generally in separate locations, making distance a limiting factor. Also, these units are typically licensed by different technology providers who are unwilling to integrate their units due to process risks.

Fig. 8 presents the composite curves for the new flow sheet where the cryogenic ASU was replaced with the ITM oxygen unit. Note that now the streams of the ITM oxygen unit requiring heating and cooling are *included* in the composite curve analysis. A ΔT_{min} of 30 °C was obtained. This shows that integrating the ITM oxygen has potential to significantly reduce the temperature driving force, compared to the conventional method of cooling syngas. It is evident from the figure that the syngas cooling from 1033 °C and air heating up to 900 °C can be matched, and therefore no external heat source is required. The minimum cooling target was found to be 58 MW and the heating target still zero.

3.4. Methanol turbine expander integration

Fig. 9 presents the composite curves for the conventional methanol synthesis flow sheet, Case A/B. The results show that the methanol synthesis is already subjected to adequate thermal integration via the feed/effluent heat exchange over the reactor. The actual cooling is equal to the minimum cooling target of 108 MW.

Fig. 10 shows the integrated methanol process gas power cycle, Case C. Reactor gas feed and effluent become the working fluids of the process power cycle where the heat of the exothermic methanol reaction is recovered by expanding the hot reactor effluent in a turbine generator to produce power. This results in reduced available process heat for feed preheating requiring further preheating using an external hot utility source. An additional compressor is also required to compress the recycle stream to the reactor pressure. The composite curves for this integrated system are presented in Fig. 11. With a minimum approach temperature of 20 °C, the minimum heating and cooling targets are 8 MW and 107 MW, respectively. These are similar to the actual heating and cooling duties showing that the process is already well integrated.

4. Results and discussion

4.1. Model validation, mass balance and process conditions

Table 3 shows the syngas composition from the simulation model for comparison to the results obtained by Venter (2002). The results compared well with each other. A deviation that is within 10 % was noted. The ATR temperature in this work was increased to 1033 °C which is still within typical ATR operating temperatures (Blumberg et al., 2017). The final syngas composition is presented in Table 4. Table 5 shows the syngas conversion to methanol results. The conversion was compared to the work of Lucking (2017) where a 9 % deviation was noted. The results of this work were further validated by

Table 8
Heat and work.

Case		A	B	C
Heat (MW)				
Q_{HT1}	ATR feed preheating	60	60	60
Q_{WHB}	Syngas waste heat boiler	133	-	-
Q_{WHB1}	Syngas waste heat boiler 1	48	48	48
Q_{HPPH}	BFW preheat for HP steam	52	-	-
Q_{HPSUP}	Fired heat for HP superheat	32	-	-
Q_{HP}	Total heat into HP cycle	217	-	-
Q_{AH}	Syngas ITM air heater	-	133	133
Q_{HT2}	BFW preheat for process steam	29	29	29
Q_{HT6}	Process steam superheat	4	4	4
Q_{HT3}	Syngas preheat to MR	75	75	66
Q_{HT8}	Additional syngas preheat	-	-	8
Q_{MR}	Reaction heat to MP steam	163	163	163
Q_{MPPH}	BFW preheat for MP steam	24	24	24
Q_{MPSUP}	Fired heat for MP superheat	30	30	30
Q_{MP}	Total heat in MP cycle	217	217	217
Work (MW)				
Compressors				
W_{ASU}	Cryogenic ASU	32(1)	-	-
W_{AC}	ITM air comp	-	61	61
W_{OC}	ITM oxygen comp	-	13	13
W_{SGC}	Syngas comp	30	30	30
W_{MRC}	Recycle comp	-	-	6
Expanders				
W_{NT}	Reject expander	-	80	80
W_{OT}	Oxygen expander	-	22	22
W_{HPST}	HP steam	51	-	-
W_{MPST}	MP steam	30	30	30
W_{MT}	Methanol gas expander	-	-	10
Total				
W_{REF}	Reformer block	19	28	28
W_{MET}	Methanol block	0	0	4
W_{TOTAL}	Plant total net	19	28	32

(1) Beysel (2009).

comparison of certain performance factors to other studies as discussed below.

Table 6 shows the mass balance and process conditions for case A, B and C. Specific methane consumption for methanol production in case A, B and C, which was found to be 0.52, 0.52 and 0.53 t_{CH3}/t_{CH3OH} respectively, is similar to the specific methane consumption of 0.54 t_{CH3}/t_{CH3OH} reported by Blumberg et al. (2016). A slightly lower (2 %) methanol production in case C can be attributed to a lower flash pressure of 70 bar in the liquid knockout drum DM2 shown in Fig. 10. The lower pressure is caused by turbine expansion of the methanol reactor effluent. To mitigate this effect, a lower flash temperature in DM2 is required.

Only 12 % of the natural gas feed is used as utility fuel in the conventional ATR-based flow sheet, case A. This is an improvement over the SMR-based methanol process which reportedly consumes 20 % (Stanbridge, 2016). From case A to case B, elimination of the HP steam cycle led to a reduction in the utility natural gas consumption from 16.8 t/h to 6.8 t/h and a corresponding reduction in CO_2 emissions. From case B to case C, a slight increase in the natural gas from 6.8 to 7.5 t/h is noted as a result of the additional reactor feed preheater HT8.

4.2. Energy analysis

Definitions for thermal efficiencies are given in Table 7. Table 8 and Table 9 show the energy analysis results, including efficiencies. Syngas from the ATR is used to heat the air feed to the ITM oxygen unit. After air is heated, there is still enough heat to generate the amount of steam required for process use. Integration of ITM oxygen membranes provides the opportunity to configure a CHP system where the syngas heat is used in a high temperature cycle and then still recover useful heat on the low temperature side. The resulting elimination of fired HP BFW preheater and steam superheater is a benefit in terms of capital investment, carbon emissions and utility requirements.

60 MW of heating utility is required to preheat the ATR feed. Although theoretically this is not required, the conventional preheating of the ATR feed via a fired heater was maintained through all the cases. Again, in the methanol synthesis loop, the conventional feed/effluent heat exchanger HT3 concept is maintained. The lower duty of HT3 in Case C is supplemented by an additional 8 MW source of heat to achieve the same preheating requirement for the feed gas to the methanol reactor. This is caused by the reduction in the product heat available for preheating after expansion in the methanol expansion turbine. A similar observation was also made by Kotowicz et al. (2022) and Azadi et al. (2016).

All cases can produce enough power to drive the compressors and pumps, with some excess power. The excess power can be supplied to other units on the plant, such as the product upgrading units. Case A can generate power in excess of 19 MW. Note that the Cryogenic ASU power requirement is included in case A. This was based on the specific power consumption of 0.33 kWh/Nm^3 (Beysel, 2009). As a result of the integrated ITM oxygen power cycle, case B can generate power in excess of 28 MW, indicating an overall power production improvement of 47 % compared to case A. With the further integration of a turbine expander in the methanol synthesis loop in case C, 32 MW excess power can be produced, resulting in overall 68 % power production improvement compared to case A. Note that power consumption by the pumps in the steam cycles are considered negligible as these vapour-liquid cycles have very low back work ratios, in the order of 1%.

The efficiency of combined process steam, oxygen and power generation was defined to enable comparison of the CHP systems in case A and case B/C. Figs. 12 and 13 show schematic diagrams with the system boundaries where process steam is generated using the smaller waste heat boiler (WHB1) downstream of the main waste heat boiler (WHB) in case A or air heater (AH) in case B/C, using syngas heat.

The heat input for the methanol process gas power cycle, and integrated MP steam cycle, is provided by the heat of reaction in the methanol reactor. The MP steam is further superheated in a fired heater. The performance of this system is expressed in terms of the lower heating value (LHV) efficiency to account for the methanol energy content.

Thermal efficiencies for the HP and MP steam cycles were found to be 23 % and 14 %, respectively. Typical Rankine cycle thermal efficiencies of 33 % are reported in literature (Ramireddy, 2012). The ITM oxygen cycle in Fig. 7 was found to have a thermal efficiency of 21 % which is lower than the typical gas turbine cycle efficiency of 44.7 % (Langston, 2020). The process requirement for oxygen at 24 bar contributes to this low efficiency. The HP steam and ITM gas power cycle thermal efficiencies are very similar. Only when we consider the combined power, oxygen production and steam (heat) efficiencies, a difference is noted. The thermal efficiency of the combined process steam, power and oxygen production as configured in Fig. 12 (Case A) and Fig. 13 (Case B/C) were found to be 22 % and 41 %, respectively.

Case C in Fig. 10 shows the methanol synthesis process configured as a heat engine. This is a combined gas and steam turbine cycle, where heat from the gas turbine cycle is transferred to the steam cycle through the methanol reactor instead of a heat recovery steam generator (HRSG) as in a typical combined power cycle. The low thermal efficiency of this cycle can be attributed to the large pressure ratio across the syngas compressor (SGC) of 3.75 which is a process requirement and the low gas turbine pressure ratio of 1.3, as well as the lower turbine inlet temperature of 280 °C.

The carbon efficiency for case A was found to be comparable to typical GTL carbon efficiencies. An improvement in the overall carbon efficiency was observed in case B and C, mainly due to the reduction in usage of natural gas as utility fuel gas. It was found that the specific gas

Table 9
Power cycle thermal and plant LHV efficiencies.

Case	A	B	C	Literature
Cycle thermal efficiency (%)				
MP Rankine steam cycle	14	14	14	33(1)
HP Rankine steam cycle	23	-	-	33(1)
ITM oxygen Brayton cycle	-	21	21	44.7(7)
ASU combined power and steam	22	-	-	
ITM cycle combined power and steam	-	41	41	
Methanol combined gas and steam cycle	-	-	2	
LHV efficiency (%)				
Reforming block	92	92	92	70(2)
Methanol block	87	87	88	
Total process	79	79	79	
Total plant	69	75	75	75(3)
Carbon efficiency (%)				
Reforming block	98	98	98	
Methanol block	93	93	93	89–95(4)
Total process	91	91	91	
Total plant	81	87	86	77(6)
Specific gas efficiency (GJ/t methanol)				
Total plant	31	29	29	37–39(4)
CO_2 emissions (t/t methanol)				
Total plant	0.25	0.14	0.15	0.462–0.881(5)
Fuel gas split (%)				
Natural gas to process	88	5	95	80(4)
Natural gas to utilities	12	4.8	4.8	20(4)

(1) Ramireddy (2012).
(2) Khan et al. (2020).
(3) Matzen et al. (2015).
(4) Stanbridge (2016).
(5) Kajaste et al. (2018).
(6) Dong et al. (2008).
(7) Langston (2020).

efficiency of the ATR-based methanol process modelled in this study was slightly lower than the 37–39 GJ/t methanol range (Stanbridge, 2016) reported for SMR-based methanol processes. A specific natural gas efficiency of 31 GJ/t methanol was obtained for case A. Case B and C specific gas efficiency improved by 6 % compared to case A. Waste CO_2 is produced from combustion of utility fuel and from the ATR. The waste CO_2 in case A was found to be lower than that reported by Kajaste (2018) and the Methanol Institute (2023). The exclusion of waste CO_2 generation associated with energy requirements for crude methanol distillation may be contributing to the difference. It can also be due to no syngas process heat recovery for power production. The waste CO_2 in case B and C decreased by 44 % and 40 % compared to case A.

4.3. Exergy analysis

The exergy rate balance which is made up of exergy transfer accompanying heat transfer (E_q) and work (E_w) and, exergy destruction (E_d) was applied in the calculation of equipment exergy destruction results (Moran et al., 2006):

$$0 = \sum_j E_{Qj} - W_{cv} + \sum_i E_i - \sum_e E_e - E_d \quad (13)$$

With adequately insulated equipment, heat loss to the environment and therefore exergy transfer accompanying heat transfer is negligible. The exergy balance then reduces to:

$$E_d = -W_{cv} + \sum_i E_i - \sum_e E_e \quad (14)$$

For the methanol reactor where heat is transferred to a steam system, the exergy balance reduces to:

$$E_d = \sum_j E_{Qj} + \sum_i E_i - \sum_e E_e \quad (15)$$

For other various equipment, the exergy balance reduces to:

$$E_d = \sum_i E_i - \sum_e E_e \quad (16)$$

Table 10 shows the overall exergy analysis results in each case. The results are also presented graphically in Fig. 14. Table 11 shows the exergy results for selected sections of the flow sheets. The ATR process or reforming block with a cryogenic ASU in case A was found to contribute 81 % of the total exergy loss. Iandoli and Kjelstrup, (2007) found this to be 69 % in a FT synthesis-based plant which uses the ATR and cryogenic ASU. The ATR was found to have the highest exergy destruction at 133 MW, which amounts to a 32 % of the total exergy losses, comparable to the finding of Iandoli and Kjelstrup, (2007). This exergy loss is unavoidable and is caused by the high entropy production due to chemical reactions and large temperature changes. Exergy destruction in the methanol reactor is significantly lower than that of the ATR. Blumberg et al. (2016) reported a similar finding. This can be attributed to the absence of large entropy producing chemical reactions such as the combustion reaction and lower temperature changes. Fired heaters were found to also contribute significantly to exergy destruction. This is expected as these are combustion reactors. This can be avoided if

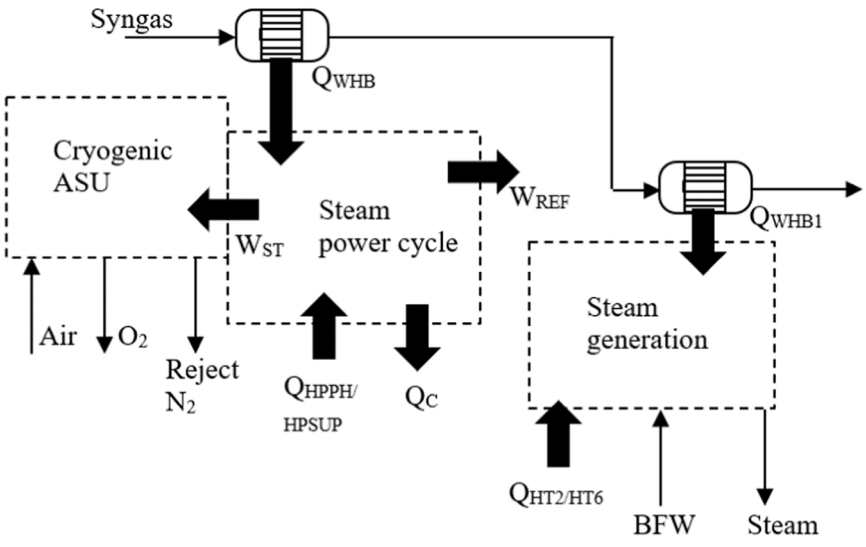

Fig. 12. Combined process steam, power and cryogenic ASU system, case A.

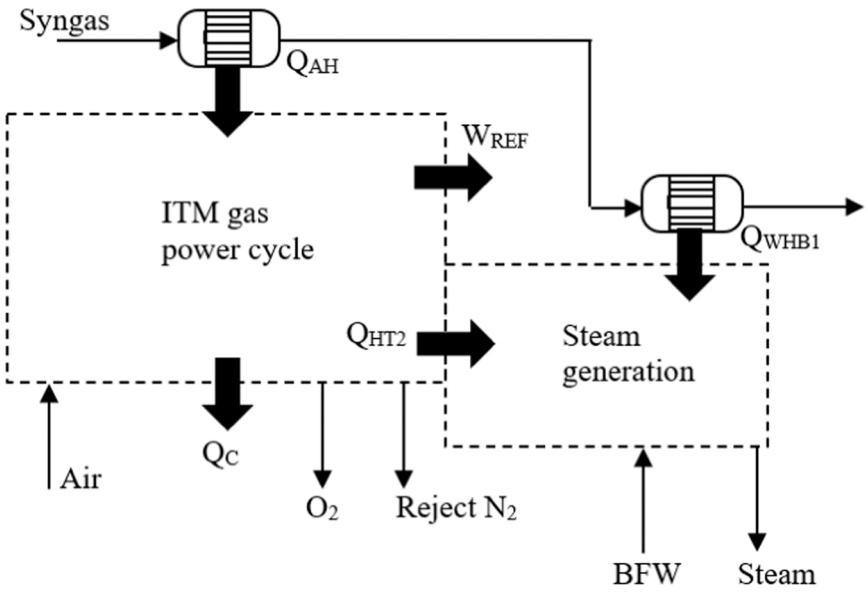

Fig. 13. Combined steam, power and ITM oxygen production system, case B and C.

Table 10
Exergy destruction over equipment.

Case	A		Iandoli and Kjelstrup (2007)	B		C	
Exergy	**MW**	**%**	**%**	**MW**	**%**	**MW**	**%**
HT1	49	12	7	58	18	58	17
ATR	134	32	33	133	41	133	40
WHB	38	9		-		-	
AH	-			15	5	15	5
WHB1	7	2		7	2	7	2
DM1	4	1		4	1	4	1
HPPH/HPSUP	87	21		-		-	
HPST	7	2		-		-	
Cryogenic ASU(1)	9	2	9	-		-	
ITM oxygen ASU	-			28	9	28	9
SGC	3	1		3	1	3	1
HT3	3	1		3	1	2	1
HT8	-			-		6	2
MR	22	5		22	7	22	7
MT	-			-		2	1
DM2	1	0		1	0	1	0
RC	-			-		2	1
MPSUP	44	11		44		44	13
MPST	5	1		5	1	5	1
Total							
Reformer + ASU block	334	81	69	246	67	246	65
Methanol block	78	19		78	24	87	26
Overall plant	411	100		323	100	333	100
Specific overall (MJ/kg_{CH3OH})	6.7			5.2		5.4	

(1) Taniguchi et al. (2015).

alternative heating methods are identified and process heat integration in the flow sheet is improved to avoid or reduce the use of fired heaters. The WHB is another significant contributor to exergy destruction, contributing 9 % to the total exergy losses in case A. This is attributed to the large temperature driving forces between the syngas at 1033 °C and water at 250 °C.

It was found that in case B, replacing the cryogenic ASU with the ITM oxygen resulted in a decrease in the overall plant exergy destruction by 21 %. In this case, the WHB is replaced by the air heater and the exergy destruction is seen to decrease from 38 MW in the WHB of case A to 15 MW in the air heater of case B. Case C overall exergy destruction decreased by only 19 % relative to case A. This slight deterioration, if compared to case B, is due to the introduction of additional equipment required to configure the methanol synthesis process into a gas turbine cycle. As a result, case C can produce more power at a slightly higher energy penalty than case B as seen from the slight increase in the exergy destruction on Table 10.

Exergy analysis results of the cryogenic ASU and HP Rankine steam cycle in case A and ITM oxygen Brayton power cycle in case B are compared. It was found that the exergy losses associated with oxygen and power production decreased from 141 MW in case A to 40 MW in case B. This shows a 72 % improvement in exergy losses for combined power and oxygen production as a result of the replacement of the cryogenic ASU and HP steam cycle with the ITM oxygen unit configured as a power cycle. The HP steam fired heater HPSUP in case A with exergy destruction of 87 MW was eliminated in case B and C. The elimination of the HP steam cycle and improvement of the temperature driving forces in the syngas cooler (WHB vs air heater), are the main reasons for the improvement in the exergy destruction in case B and C compared to case A. This confirms that replacing the cryogenic ASU with ITM oxygen and integrating the ITM oxygen into the ATR process is a more energy efficient method for combined power and oxygen production. This was found to improve the natural gas to methanol flow sheet's thermal efficiency and therefore net energy requirement, which translates to lower production costs.

5. Conclusions

New natural gas to methanol flow sheets (case B and C) were developed and compared to a conventional flow sheet (case A). Case A comprised the ATR and isothermal methanol and cryogenic ASU technologies. The new flow sheets were an extension and modification of Case A based on identified opportunities for thermal efficiency improvement. In case B, the cryogenic ASU is replaced with the novel ITM oxygen which is also heat integrated into the ATR process. In case C, the methanol synthesis process is configured into a gas turbine cycle. The flow sheets were constructed and modelled in Aspen Plus V10. An analysis of the energy and exergy results was performed, and the results were compared.

It was found that is possible to replace the cryogenic ASU with the ITM oxygen for oxygen production. There is enough process syngas heat available to provide the ITM oxygen unit heating requirement and to

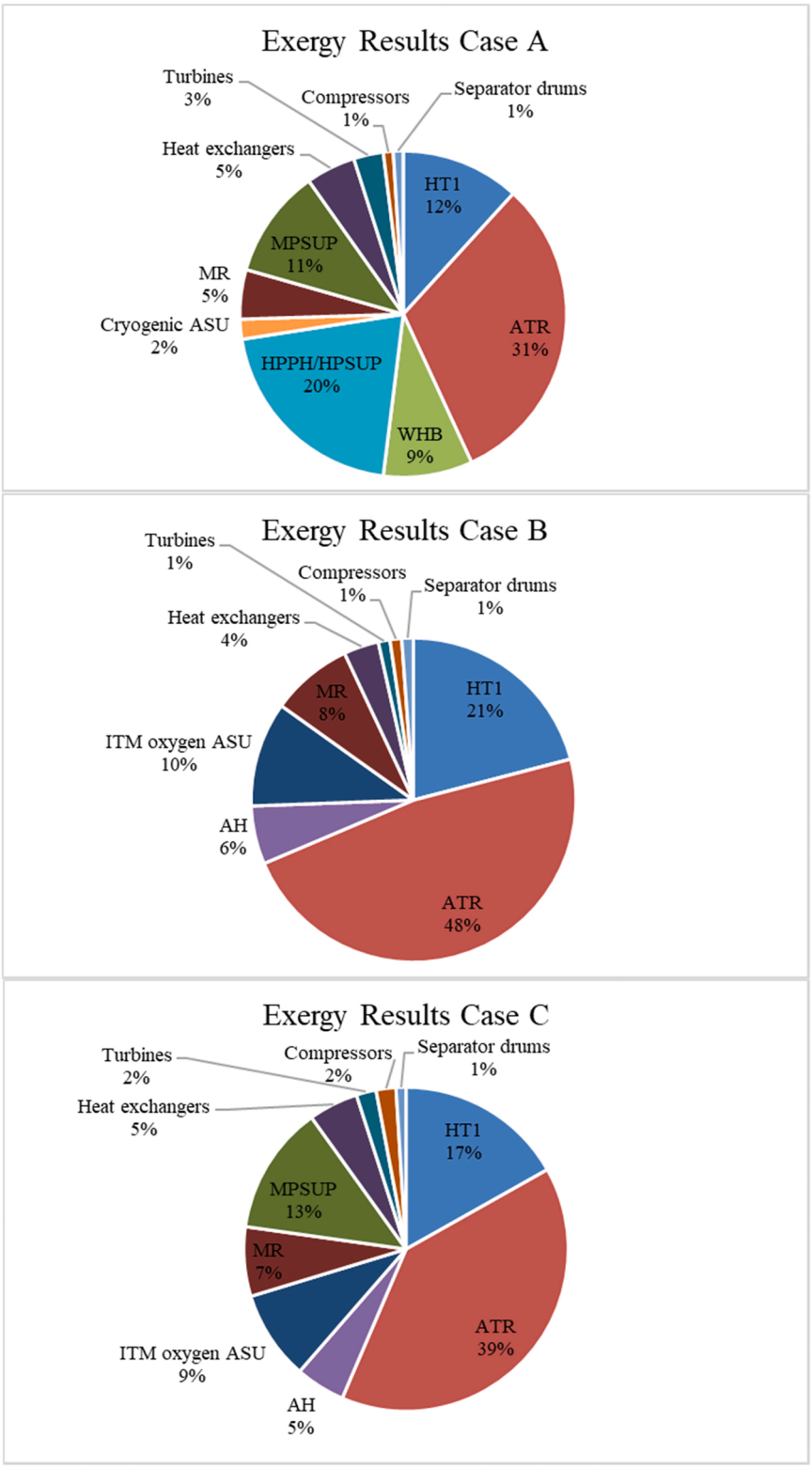

Fig. 14. Exergy destruction over equipment for case A, B and C.

generate process steam feed for the ATR. All cases produced enough power to satisfy its internal demand, with some excess power. It was found that power production improved by 47 % in case B and 68 % in case C compared to case A.

A thermal efficiency definition suitable for combined process steam, power and oxygen production was used to compare the cryogenic ASU combined oxygen, power and process steam system in case A, to the ITM oxygen combined oxygen, power and process steam system in case B and C. The results showed a 22 % efficiency in case A and 41 % efficiency in case B and C. Case A was found to consume only 12 % natural gas as utility fuel which is lower than SMR-based methanol processes. This reduced to about 5 % in case B and C.

Decreases in the overall plant exergy losses by 21 % in case B and 19 % in case C were found. From case B to C, a slight increase in the energy

Table 11
Exergy destruction of components of the HP steam and ITM oxygen power cycles.

	Unit	Case A	Case B
ITM oxygen ASU and power cycle			
AC	MW	-	13
OC	MW	-	3
NT	MW	-	7
OT	MW	-	2
AH	MW	-	15
Cryogenic ASU and HP steam cycle			
Cryogenic ASU(1)	MW	8.6	-
HPST	MW	7	-
WHB	MW	38	-
HPPH/HPSUP	MW	87	-
Total	MW	**141**	**40**

(1) Taniguchi et al. (2015).

penalty is found as a result of introducing the methanol syngas turbine cycle equipment. Case B and C present an improved method for power and oxygen production in large-scale natural gas to methanol flow sheet with reduced energy penalties and higher thermal efficiencies, therefore reduced net energy requirement, which translates to lower production costs when compared to the conventional flow sheet.

Declaration of Competing Interest

The authors declare that they have no known competing financial interests or personal relationships that could have appeared to influence the work reported in this paper.

References

Aasberg-Petersen, K., Stub Nielsen, K., Dybkjær, I., Perregaard, J., 2022. Large-scale Methanol Production from Natural Gas. Accessed on 10 June. Haldor Topsøe Publication,, Lyngby, Denmark. ⟨https://www.researchgate.net/profile/Rick_Manner/post/CO2_Hydrogenation_to_produce_methanol_model_simulation/attachment/59d650a279197b80779a963d/AS %3A503928378884096 %4014971572 96471/download/Topsoe_large_scale_methanol_prod_paper.pdf⟩.

Air Liquide, Air Liquide supports the development of the largest Methanol plant in Africa, published 5 March 2021, accessed 2 April 2022. ⟨https://www.engineering-airliquide.com/air-liquide-supports-development-largest-methanol-plant-africa#:~:text=This %20Methanol %20plant %2C %20to %20be,methanol %2C %20Lurgi %20MegaMethanol %E2 %84 %A2 %2C %20which⟩.

Anderson L.L., Armstrong P.A., Repasky J.M. and Stein V.E., Enabling clean coal power generation: ITM oxygen technology, International Pittsburgh Coal Conference. Pittsburgh: Air Products and Chemicals, Inc, 2011.

Anderson, L.L., Armstrong, P.A., Broekhuis, R.R., Carolan, M.F., Chen, J., Hutcheon, M. D., Lewinsohn, C.A., Miller, C.F., Repasky, J.M., Taylor, D.M., Woods, C.M., 2016. Advances in ion transport membrane technology for oxygen and syngas production. Solid State Ion. 288, 331–337.

Azadi, M., Tahouni, N., Panjeshahi, M.H., 2016. Energy conservation in methanol plant using CHP system. Appl. Therm. Eng. 107, 1324–1333.

Bai, W., Feng, J., Luo, C., Zhang, P., Wang, H., Yang, Y., Zhao, Y., Fan, H., 2021. A comprehensive review on oxygen transport membranes: development history, current status, and future directions. Int. J. Hydrogen Energy 46, 36257–36290.

Balopi, B., Danha, P.A., 2019. Methanol synthesis chemistry and process engineering aspects - A review with consequences to Botswana chemical industries. Procedia Manuf. 367–376.

Beysel G., 2009, Enhanced cryogenic air separation. A proven process applied to oxyfuel-Future Prospects, 1st *Oxyfuel Combustion Conference*, The Linde Group, accessed on 5 July 2021. ⟨https://ieaghg.org/docs/oxyfuel/OCC1/Plenary %201/Beysel_ASU_1st Oxyfuel %20Cottbus.pdf⟩.

Blumberg T., Morosuk T., and Tsatsaronis G., 2016, Exergy-based evaluation of methanol production from natural gas, Research Gate, conference paper, ⟨https://www.researchgate.net/publication/320271856_Exergy-based_evaluation_of_methanol_production_from_natural_gas⟩ [accessed 7 Aug 2022].

Blumberg, T., Morosuk, T., Tsatsaronis, G., 2017. A comparative exergo-economic evaluation of the synthesis routes for methanol production from natural gas. Appl. Sci. 7 (12), 1213.

Brelsford, R., 2020. Turkmenistan commissions new methanol plant. Oil Gas. J. ⟨https://www.ogj.com/refining-processing/article/14074727/turkmenistan-commissions-new-methanol-plant⟩ 14 January.

Den Exter, M.J., Haije, W.G., Vente, J.F., 2009. Viability of ITM technology for oxygen production and oxidation processes: material, system, and process aspects. In: Bose, A.C. (Ed.), Inorganic Membranes for Energy and Environmental Applications. Springer, New York, NY.

Dong, L., Wei, S., Tan, S., Zhang, H., 2008. GTL or LNG: which is the best way to monetize stranded natural gas? Pet. Sci. 388–394.

Fischer, C.D., Iribarren, O.A., 2017. Oxygen integration of autothermal reforming of ethanol with oxygen production, through ion transport membranes in countercurrent configuration. Comput. Chem. Eng. 99, 245–254.

Greeff I.L., 2015. Process for co-production synthesis gas and power, US Patent US9021814B2, assigned to Sasol Technology (Propriety) Limited, Johannesburg, 5 May.

Greeff I.L., 2004. Recovery of work from exothermic chemical reaction systems by means of turbine expansion, Ph.D. of Engineering Thesis, University of Eindhoven.

Greeff, I.L., 2020. Integration of a turbine expander with syngas process - using process gas as a working fluid. Appl. Therm. Eng. 165, 114574.

Greeff, I.L., 2022. Using synthesis gas heat to produce work via an externally fired gas power cycle. Energy 239, 122132.

Greeff, I.L., Visser, J.A., Ptasinski, K.J., 2002. and Janssen FJJG, Utilisation of reactor heat in methanol synthesis to reduce compressor duty - application of power cycle principles and simulation tools. Appl. Therm. Eng. 22, 1549–1558.

Habib M.A.M. and Mokheimer E.M.A., 2017. Solar power and ion transport-based enhanced oil recovery system and method, US Patent US9540918, assigned to King Fahd University of Petroleum and Minerals, Dhahran (SA), 10 January.

Iandoli, C.L., Kjelstrup, S., 2007. Exergy analysis of a GTL process based on low temperature slurry FT reactor technology with a cobalt catalyst. Energy Fuels 21, 2317–2324.

Kajaste, R., Hurme, M., Oinas, P., 2018. Methanol-Managing greenhouse gas emissions in the production chain by optimizing the resource base. AIMS Energy 6, 1074–1102.

Khan, M.N., Cloete, S., Amini, S., 2020. Efficient production of clean power and hydrogen through synergistic integration of chemical looping combustion and reforming. Energies 13, 3443.

Kiebach, R., Pirou, S., Martinez Aguilera, L., Haugen, A.B., Kaiser, A., Hendriksen, P.V., Balaguer, M., García-Fayos, J., Serra, J.M., Schulze-Küppers, F., Christie, M., Fischer, L., Meulenberg, W.A., Baumann, S., 2022. A review on dual-phase oxygen transport membranes from fundamentals to commercial deployment. J. Mater. Chem. A 10, 2152–2195.

Kotowicz, J., Brzeczek, M., Walewska, A., Szykowska, K., 2022. Methanol Production in the Brayton Cycle. Energies 15, 1480. https://doi.org/10.3390/en15041480.

Langston, L.S., 2020. Aspects of gas turbine thermal efficiency. ASME, Mech. Eng. 142, 54–55.

Lucking L.E., 2017. Methanol production from syngas, process modelling and design utilization biomass gasification and integration hydrogen supply, PhD Thesis, Delft university of technology.

Madloch, S., Dorcheh, A.S., Galetz, M.C., 2018. Effect of Pressure on Metal Dusting Initiation on Alloy 800H and Alloy 600 in CO-rich Syngas. Oxid. Met. 89, 483–498. https://doi.org/10.1007/s11085-017-9801.

Matzen, M., Alhajji, M., Demirel, Y., 2015. Technoeconomics and sustainability of renewable methanol and ammonia productions using wind power-based hydrogen. J. Adv. Chem. Eng. 5, 128.

Methanol Institute, Carbon Footprint of Methanol, published 31 January 2022, accessed 5 August 2023. chrome-extension://efaidnbmnnnibpcajpcglclefindmkaj/https://www.methanol.org/wp-content/uploads/2022/01/CARBON-FOOTPRINT-OF-METHANOL-PAPER_1–31-22.pdf.

Miller, C.F., Chen, J., Carolan, M.F., Foster, E.P., 2014. Advances in ion transport membrane technology for syngas production. Catal. Today 228, 152–157.

Mitsubishi Gas Chemical, Methanol, accessed 5 May 2022. https://www.mgc.co.jp/eng/products/nc/methanol.html.

Portillo, E., Alonso-Fariñas, B., Vega, F., Cano, M., Navarrete, B., 2019. Alternatives for oxygen-selective membrane systems and their integration into the oxy-fuel combustion process: a review. Sep. Purif. Technol. 229, 115708.

Ramireddy V., 2012, An overview of combined cycle power plant, Electrical Engineering Portal. ⟨https://electrical-engineering-portal.com/an-overview-of-combined-cycle-power-plant⟩ (Accessed 21 September 2022).

Rao P. and Muller M., 2007. Industrial Oxygen: Its Generation and Use, *ACEEE Summer study on Energy Efficiency in Industry*, The State University of New Jersey.

Smit R., Sprachman G., 2016. Process for the preparation of syngas, *WO2016/074976A1*, Shell Internationale Research Maatschappij B.V, The Hague, 19 May.

Stanbridge S., 2016. Teaching an old plant new tricks: The rise of the methanol plant revamp, Hydrocarbon Processing, 1 July. https://www.hydrocarbonprocessing.com/magazine/2016/july-2016/special-report-refinery-of-the-future/teaching an old plant new tricks: The rise of the methanol plant revamp.

Sunarso, J., Baumann, S., Serra, J.M., Meulenberg, W.A., Liu, S., Lin, Y.S., Diniz da Costa, J.C., 2008. Mixed ionic–electronic conducting (MIEC) ceramic-based membranes for oxygen separation. J. Membr. Sci. 320, 13–41.

Taniguchi, M., Asaoka, H., Ayuhara, T., 2015. Energy Saving Air-separation Plant Based on Exergy Analysis, KEBELCO Technology Review No. 33. Shinko Air Water Cryoplant, Ltd.

Tesch S., Morosuk T., Tsatsaronis G., 2019. Comparative evaluation of cryogenic air separation units from the exergetic and economic points of view, accessed 6 August 2021. ⟨https://www.intechopen.com/books/low-temperature-technologies/comparative-evaluation-of-cryogenic-air-separation-units-from-the-exergetic-and-economic-points-of-v⟩.

Venter J.A., 2002. Modelling and exergy analysis of the natural gas to hydrocarbon liquid (GTL) process, Master of Engineering Thesis, University of Pretoria.